A high-energy inelastic neutron scattering investigation of the Gd-Co exchange interactions in GdCo4B: Comparison with density-functional calculations

Olivier Isnard, Michael D. Kuz'Min, Manuel Richter, Michael Loewenhaupt, Robert Bewley

A high-energy inelastic neutron scattering investigation of the Gd–Co exchange interactions in $GdCo_4B$: Comparison with density-functional calculations

Olivier Isnard,[1,a)] Michael D. Kuz'min,[2] Manuel Richter,[2] Michael Loewenhaupt,[3] and Robert Bewley[4]
[1]*Institut Néel, CNRS/Université de Grenoble J. Fourier, Avenue des martyrs, F-38042 Grenoble, France and Institut Universitaire de France, Maison des Universités, 103 Boulevard Saint-Michel, F-75005 Paris Cédex, France*
[2]*IFW Dresden, P.O. Box 270016, D-01171 Dresden, Germany*
[3]*Institut für Festkörperphysik (IFP), Technische Universität Dresden, D-01062 Dresden, Germany*
[4]*ISIS, Rutherford Appleton Laboratory, Chilton, Didcot, Oxon OX11 0QX, United Kingdom*

(Received 16 February 2008; accepted 6 May 2008; published online 14 July 2008)

Inelastic neutron scattering is used to quantify the Gd–Co exchange interaction in $GdCo_4B$. A significant reduction is observed in comparison with the $GdCo_5$ compound. A mean value of 130 T is obtained for the exchange field on the two Gd sites in $GdCo_4B$. The experimental results are compared with density-functional calculations. The local atomic magnetic moments calculated using the LSDA+U approximation are reported for each atomic site of the $GdCo_4B$ crystal structure. These calculations demonstrate that the two nonequivalent Gd crystal sites experience a significantly different exchange interaction, a difference that is discussed in the light of the local atomic environment. The observed reduction of the exchange field occurring upon substituting B for Co in $GdCo_5$ is mainly caused by the decrease of the Co magnetic moment, whereas the Gd–Co coupling constant is found to be almost the same in both $GdCo_5$ and $GdCo_4B$. © *2008 American Institute of Physics*. [DOI: 10.1063/1.2953099]

I. INTRODUCTION

Intermetallic compounds based on rare-earth (R) and transition metal (T) form an important class of materials exhibiting numerous applications such as permanent magnets, magnetostrictive devices, or magneto-optical recording. The outstanding magnetic properties of these materials result from the combination of the different magnetic features of the localised 4f electronic states of the rare earth and the itinerant 3d states of the transition metal. Naturally, a key role in these combined systems is played by the 3d-4f exchange interaction, which mediates the interplay of the two magnetic subsystems. It is therefore of major interest to study this interaction quantitatively. The exchange interaction between the R and T magnetic moments is indirect and involves both intra-atomic interaction between the 4f and 5d states of the R element and interatomic interaction between the 3d and 5d spins. It is thus not straightforward to know *a priori* the magnitude of these R-T interactions, especially when several nonequivalent R sites are present in the structure.

Several experimental procedures can be used to access the intersublattice exchange interaction.

(i) Phenomenological analysis of Curie temperature in a series of isotype compounds with magnetic as well as nonmagnetic R.[1–6] This method is general but has proved to be inaccurate.
(ii) Fitting the experimental thermal dependence of the magnetization with a Brillouin function can also be used,[6] leading to a rough estimation of the molecular field coefficients.
(iii) High field free-powder method has also been used extensively.[7–9] High field measurements on free single-crystalline spheres are more accurate.[10]
(iv) When single crystals are available, the intersublattice coupling strength can be derived by analyzing the low temperature magnetic isotherms measured along the main crystallographic axis.[11]
(v) Rare-earth elements having suitable Mössbauer nuclei can also be used.[12] This method is however restricted to a limited number of rare-earth elements.
(vi) Finally, inelastic neutron scattering can be used[13,14] as a direct measurement of the exchange field experienced at the Gd site in Gd containing compounds.[14–16] The exchange field can also be derived from intermultiplet transitions in Sm.[17,18]

Density-functional calculations have been employed to evaluate the intersublattice exchange interaction at the rare-earth site.[19,20] Recently, this method has been successfully used in the $GdCo_5$ compound[10] and results have been compared with high field measurements on single crystal.

Here we report on results of inelastic neutron scattering experiments on $GdCo_4B$ and related density-functional calculations of the Gd–Co exchange interactions. The purpose of the present study is first to investigate the effect of boron for cobalt substitution on the Gd–Co exchange interaction by comparison of the $GdCo_4B$ and $GdCo_5$ compounds and sec-

a)Electronic mail: olivier.isnard@grenoble.cnrs.fr.

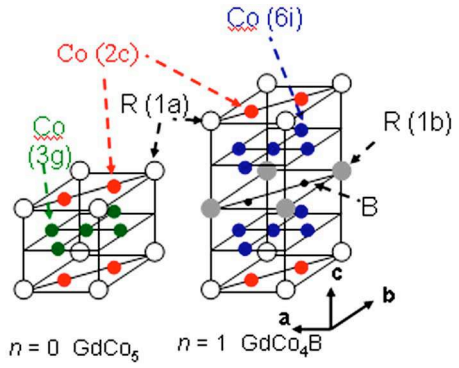

FIG. 1. (Color online) Comparison of the $GdCo_5$ and $GdCo_4B$ crystal structures.

ond to probe the effect of the local atomic environment on the exchange interaction experienced at nonequivalent Gd crystal sites.

Indeed it is possible to substitute boron for cobalt in RCo_5 to obtain the family of compounds $R_{n+1}Co_{3n+5}B_{2n}$, with $n=0,1,2,3,\infty$, which form a unique series of crystal structures changing with n.[21] All these structures are derived from the $CaCu_5$-type structure and can be described by an ordered substitution of B for Co in RCo_5. Consequently, these compounds are excellent candidates for investigating the magnetic properties of the Co and R sublattice in the *R-T-B* intermetallics. In the $R_{n+1}Co_{3n+5}B_{2n}$ system the ordering temperature and the Co moment decrease dramatically as n increases.[22–25] The Curie temperatures of $Y_{n+1}Co_{3n+5}B_{2n}$ are 985, 380, 345, and 310 K for $n=0$, 1, 2, and 3 respectively. The compound YCo_3B_2 ($n=\infty$) is even paramagnetic at all temperatures.[23,26]

As can be seen from Fig. 1, the series RCo_4B ($n=1$) is obtained by the ordered substitution of boron for cobalt in every second layer of the RCo_5 structure. An important example is the compound $SmCo_4B$, which exhibits some characteristics of a hard magnetic material.[23,27]

II. EXPERIMENTAL DETAILS

A. Sample preparation

The polycrystalline $GdCo_4B$ sample was prepared in an arc furnace and then remelted by induction melting technique. Both meltings have been performed in a cold copper crucible under argon atmosphere, using elements of purity better than 99.95% for gadolinium and for cobalt. The boron used was ^{11}B from Euriso-Top S.A.[28] In order to improve the sample homogeneity and crystallization, small segments of the resulting ingot were wrapped in tantalum foil, sealed in an evacuated silica tube, annealed at 1173 K for two weeks, and then water quenched.

Sample quality was tested by thermomagnetic measurements. Only one magnetic transition has been observed, indicating that the sample is single phase. This result has been confirmed using x-ray diffractometry. The homogeneity of the sample was checked by conventional x-ray powder diffraction with copper $K\alpha$ radiation. High accuracy lattice parameters were determined with a Guinier-type focusing camera equipped with a monochromatic x-ray beam containing only $K\alpha_1$ radiation. Silicon was added to the powder sample and used as an internal standard. The diffraction patterns were recorded on x-ray film that was subsequently scanned with 20 μm steps in order to extract the relative diffraction intensities. The indexing of the Bragg peaks was performed on a hexagonal unit cell compatible with the $P6/mmm$ space group. The lattice parameters were then obtained by a least squares refinement using all the 25 observed Bragg reflections: $a=5.058(2)$ Å and $c=6.892(2)$ Å.

B. Inelastic neutron scattering

The experiment was performed on the high-energy transfer (HET) spectrometer at the UK spallation neutron source ISIS of the Rutherford Appleton Laboratory. HET is a direct geometry chopper spectrometer[29] equipped with four ^3He detector banks, one lying at 4 m from the sample and covering a full scattering angle range $\varphi=3°-7°$, and another is located at 2.5 m from the sample and spans an angular range of 10°–30°. The other two provide data at large angles, $\varphi=115°$ and $\varphi=135°$. Incident energies from 30 to 2000 meV may be selected at the sample position by phasing a Fermi chopper to the 50 Hz source proton pulse. The neutron flux and resolution of the spectrometer can be varied by choosing different slit packages and rotation frequencies (in multiples of 50 Hz) for the chopper. This gives a wide choice of experimental configurations with high-energy resolution and small scattering vector Q. The scattering function $S(Q,\omega)$ is obtained by sorting the signals from the detectors according to the scattering angle and the neutron time of flight. In the present experiment, the frequency of the Fermi chopper was set to its maximum value of 600 Hz. This has led to a full width at half maximum of about 8 meV. Correction for the efficiency of the detectors was done using the scattering of a neutron white beam with a vanadium sample as standard. The $GdCo_4B$ sample consisted of approximately 15 g of polycrystalline powder mounted in aluminum can onto the cold plate of a closed-cycle refrigerator. Measurements were performed at 15 K with an incident energy of 250 meV. At 15 K, the $GdCo_4B$ sample was magnetically ordered and can be considered as carrying its fully saturated magnetization. The specimen was prepared using Gd with natural isotopic composition, even though the presence of the strong ^{155}Gd and ^{157}Gd neutron absorption cross sections is not favorable. However, with the chosen incident energy, both incident and scattered neutrons have an absorption cross section sufficiently small to allow the observation of magnetic excitations up to 50 meV. Note that ^{11}B isotope was used instead of natural boron in order to achieve a reasonable absorption cross section.

C. Calculation method

The intersublattice exchange field on both Gd sites was computed using the standard approach.[30] Three independent self-consistent electronic structure calculations were carried out, one for each of the following three spin structures.

(0) The ferrimagnetic ground state: The moments of both

Gd($1a$) and Gd($1b$) are antiparallel to those of the joint cobalt sublattice Co($2c$)+Co($6i$). This was the reference state.

(1) Excited state 1: The moments of Gd($1a$) reversed with respect to the ground state.

(2) Excited state 2: The moments of Gd($1b$) reversed with respect to the ground state.

The energy differences associated with the moment reversal, E_1-E_0 and E_2-E_0, are directly proportional to the exchange fields on Gd($1a$) and Gd($1b$), respectively. The difficulty which usually arises when mapping such calculations onto a model is that the corresponding proportionality relations, e.g., $2B_a\mu_a=E_1-E_0$, contain a single value of the magnetic moment, whereas two different sets of magnetic moments are obtained in the calculations for the two states involved. The usual way out is to average the moment being reversed, so as to obtain the required proportionality factor, and to ignore the fact that the reversal affects the values of all the other moments. That the change of the cobalt moments cannot be simply disregarded is particularly easy to see in the mean-field approximation, $B_a=\lambda_a\mu_{\mathrm{Co}}$ and $B_b=\lambda_b\mu_{\mathrm{Co}}$, where $\mu_{\mathrm{Co}}=2\mu_c+6\mu_i$ is the moment of the cobalt sublattice.

The transition studied in our inelastic neutron scattering (INS) experiments is that between the ground state (the projection of the Gd spin on the exchange field direction is maximum) and an excited state where that projection has been incremented by −1. In a classical picture this corresponds to a rotation of the Gd spin through a small angle away from the ground-state position. Clearly, in this case the ground-state value of μ_{Co}, μ_{Co0}, should be used in conjunction with the above proportionality relations $B_a=\lambda_a\mu_{\mathrm{Co0}}$ and $B_b=\lambda_b\mu_{\mathrm{Co0}}$.

In contrast to the experimental case, the transitions between the spin structures considered in the calculations, (0) $\rightarrow$(1) and (0)$\rightarrow$(2), correspond to a 180° rotation of the Gd spins. This is not a small deviation from the ground state and the accompanying change of the cobalt sublattice moment should not be neglected. Therefore, the arithmetical mean values for spin structures 0 and 1, $\mu_{a01}=\frac{1}{2}(\mu_{a0}+\mu_{a1})$ and $\mu_{\mathrm{Co01}}=\frac{1}{2}(\mu_{\mathrm{Co0}}+\mu_{\mathrm{Co1}})$, should enter in the relation for the energy difference, $E_1-E_0=2\lambda_a\mu_{\mathrm{Co01}}\mu_{a01}$. Similarly, $E_2-E_0=2\lambda_b\mu_{\mathrm{Co02}}\mu_{b02}$, where $\mu_{b02}=\frac{1}{2}(\mu_{b0}+\mu_{b2})$.

Thus, a more consistent approach to computing the exchange field on Gd is to use the expressions $B_a=[\mu_{\mathrm{Co0}}/\mu_{\mathrm{Co01}}](E_1-E_0)/(2\mu_{a01})$ and $B_b=[\mu_{\mathrm{Co0}}/\mu_{\mathrm{Co02}}](E_2-E_0)/(2\mu_{b02})$. The prefactor in square brackets is what makes them different from the usual ones, which ignore the difference between μ_{Co0} and μ_{Co01} or μ_{Co02}. These improved expressions were employed in the present work.

The magnetic moments and total energies E_0, E_1, E_2 were obtained in scalar-relativistic electronic structure calculations using the full-potential local-orbital code (FPLO 4.00-16).[31] The mesh in reciprocal space consisted of 133 $\boldsymbol{k}$ points within the irreducible wedge of the Brillouin zone. The exchange and correlation potential in the local spin density approximation (LSDA) was taken in the form proposed by Perdew and Wang.[32] The calculations were performed at the LSDA equilibrium structure parameters $a=4.907$ Å, $c=6.737$ Å, and $z_{6i}=0.2854$. (Additional calculations using the experimental structure data, $a=5.058$ Å, $c=6.892$ Å, and $z_{6i}=0.283$, yielded much higher values of the exchange field on the Gd sites: $B_a=183$ T and $B_b=156$ T). The valence basis states included 4f, 5spd, and 6sp of Gd, 3spd and 4sp of Co, as well as 1s, 2sp, and 3d of B, the latter playing the role of polarization states. The 4f shell of Gd was treated within the so-called LSDA+U (atomic limit) formalism,[33] with $U=6$ eV. The calculation was proven to be insensitive to the value of U within reasonable bounds.[10] Spin magnetic moments were obtained for all atomic sites. These values (for the ferrimagnetic ground state) are presented in Table IV.

TABLE I. Comparison of the spontaneous magnetization of YCo_4B and $GdCo_4B$.

Compound	M_s (μ_B/f.u.) 5 K	M_s (μ_B/f.u.) 300 K
$GdCo_4B$	3.2	0.9
YCo_4B	3.0	2.2

III. RESULTS AND DISCUSSION

Magnetic properties of $GdCo_4B$ and of isotype RCo_4B compounds have been the subject of several investigations.[34–37] $GdCo_4B$ is found to order below 503 K. The Gd and Co magnetic sublattices are coupled ferrimagnetically. At low temperatures, the Gd magnetization is dominant, whereas at high temperatures the Co sublattice magnetization is dominant. The so-called compensation temperature at which the 4f and 3d sublattice magnetizations cancel each other out amounts to 397 K.[5,6] The saturation magnetization of the cobalt sublattice is usually assumed equal to that of the Y containing isotype compound. The corresponding values are given in Table I. In the case of Co containing compounds, this is an estimation only since the magnitude of the Co magnetic moments has been shown to be very sensitive to the internal molecular field experienced at the cobalt site.[23]

A detailed investigation of isotype RCo_4B phases has been undertaken by neutron diffraction and related results have been presented elsewhere.[26,24,37,38] This investigation shows that the two inequivalent Co sites carry significantly different magnetic moments. This result has been confirmed by electronic structure calculations.[39–41] One of the interesting features of this structure (Fig. 1) is the presence of two inequivalent rare-earth sites. Their local atomic environment is described in Table II. The 1b position is found in the boron

TABLE II. Interatomic distances and number of near neighbors of the two Gd sites.

	Co 6i	Co 2c	B	Gd 1a	Gd 1b
Gd 1a	12×2.89 Å	6×3.20 Å	⋯	⋯	2×3.48 Å
Gd 1b	12×2.91 Å		6×2.89 Å	2×3.48 Å	⋯

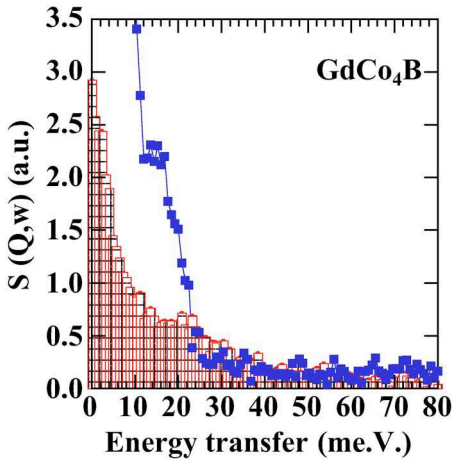

FIG. 2. (Color online) Inelastic neutron spectrum of $GdCo_4B$ as recorded at 15 K. The solid line is guide to the eyes. The shaded area indicates the nonmagnetic inelastic intensity as deduced from the spectrum recorded by the high-angle detector banks. The neutron incident energy was 250 meV.

containing plane, whereas the 1*a* site has a local environment very similar to that encountered in the RCo_5 structure type, without any boron atom as nearest neighbor.

The INS spectrum of the $GdCo_4B$ compound is shown in Fig. 2. The shaded region shows the scattering determined from the high-angle banks. This scattering is predominantly due to phonon processes as the magnetic scattering is small at such high momentum transfers.

The inelastic peak at low moment transfer can be interpreted as being due to the excitation of a dispersionless spin wave mode that corresponds to the out-of-phase precession of the Gd spins in the exchange field of neighboring spins. Consequently, from the energy of the inelastic neutron scattering signal Δ, one can derive the corresponding exchange field on the Gd sites. The latter is approximately proportional to the mean magnetic moment of cobalt because the Gd–Gd exchange interaction can be neglected in comparison with the Gd–Co one.[10]

The relation between these quantities is

$$\Delta_{a,b} = 2\mu_B B_{a,b} = 2\mu_B \lambda_{a,b} \mu_{Co0}, \quad (1)$$

where $B_{a,b}$ is the exchange field on the Gd crystal sites 1*a* and 1*b*, $\Delta_{a,b}$ is the energy of the corresponding dispersionless

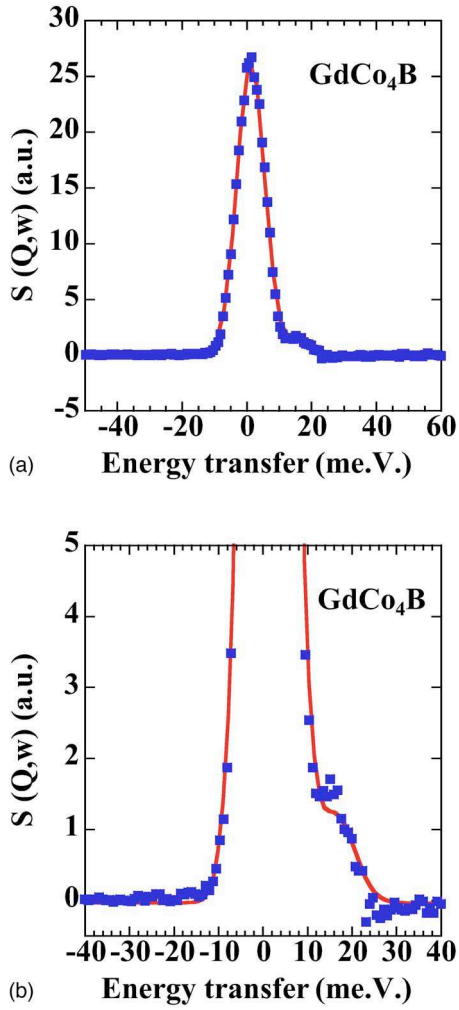

FIG. 3. (Color online) (a) Inelastic neutron spectrum of $GdCo_4B$ after removal of the nonmagnetic inelastic intensity. The points are the experimental data and the line is a fit to the data. (b) The plot represents a zoom around the inelastic signal.

modes, $\lambda_{a,b}$ are the respective molecular field constants, and μ_{Co0} represent the ground-state Co sublattice moment defined above. The values of $\lambda_{a,b}$ and $B_{a,b}$ obtained for the $GdCo_4B$ and $GdCo_5$ compounds are given in Table III.

Figure 3 displays the magnetic signal after subtraction of a nonmagnetic contribution to the background, with the line

TABLE III. Comparison of the inelastic neutron scattering results obtained in $GdCo_4B$ and in $GdCo_5$. The corresponding molecular fields on the Gd sites and Gd–Co exchange coupling constants are also reported. (The calculated mean cobalt values of μ_{Co0} represent the spin moment only.)

	$GdCo_5$			$GdCo_4B$	
	INS[a]	Magnetization[b]	LSDA+U, Calc.[b]	INS[c]	LSDA+U, Calc.[c]
Energy (meV)	27 (1)	⋯	⋯	15.0 (1.5)	⋯
B_a (T)	236 (8)	233 (12)	258	130 (10)	153
B_b (T)	⋯	⋯	⋯		134
μ_{Co0} (μ_B)	1.78	1.74	1.52	0.95	0.87
λ_a (T/μ_B)	133	134	170	137	176
λ_b (T/μ_B)	⋯	⋯	⋯		154

[a]Reference 42.
[b]Reference 10.
[c]This work.

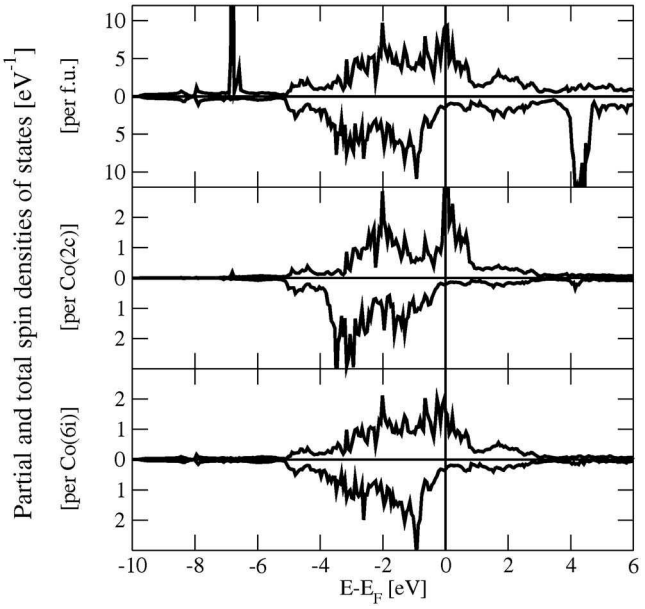

FIG. 4. Density of states of $GdCo_4B$.

corresponding to a fit of the magnetic data. The estimation of the nonmagnetic background has been deduced from the high Q values measured on the high-angle banks. The inelastic signal appears as a shoulder on the right-hand side of the high-intensity elastic line. This proximity together with the limited experimental resolution does not permit to resolve the two different INS peaks corresponding to the two nonequivalent Gd sites. The quantitative analysis of the INS data yields a value of 15 meV for the energy of the flat mode in the $GdCo_4B$ sample compared to 27 meV reported earlier for $GdCo_5$.[42] Thus, the R-T interaction has decreased: the substitution of boron for cobalt induces a reduction of the molecular field by almost a factor of 2, from 233 T in $GdCo_5$ down to 130 T in $GdCo_4B$.

The localized $4f$ and the itinerant $3d$ moments are known to interact via intra-atomic $4f$-$5d$ exchange combined with interatomic $5d$-$3d$ interaction.[21] The intra-atomic $4f$-$5d$ interaction is virtually insensitive to the chemical environment, whereas the interatomic $5d$-$3d$ coupling can be expected to be strongly affected by the boron-induced modification. As can be seen in Table III, the reduction of the exchange field $B_{a,b}$ is not induced by a reduction of the coupling constant $\lambda_{a,b}$. In contrast, the coupling constant in $GdCo_4B$ remains about the same as in $GdCo_5$. The observed decrease of $B_{a,b}$ can rather be attributed to the significant reduction of the Co magnetic moment upon the substitution of boron for cobalt (Fig. 4). Indeed, the Co magnetic moments calculated for $GdCo_4B$ (see Table IV) are much smaller than those reported for $GdCo_5$.[10] It is worth noting that the values calculated here and listed in Table IV correspond to spin only magnetic moments. These values are in good agreement both with earlier reported calculations[39] and with the experiment. Indeed, it is well known that a significant change of the magnetization takes place in the RCo_4B samples in comparison to RCo_5, predominantly in the Co sublattice.[26,24,37,38] Accordingly, the Curie temperature of $GdCo_4B$ is about one-half of that of $GdCo_5$.

TABLE IV. Calculated spin magnetic moments in $GdCo_4B$.

Notation	Atom (Wyckoff position)	Spin magnetic moment (μ_B)
μ_a	Gd ($1a$)	7.34
μ_b	Gd ($1b$)	7.28
μ_d	B ($2d$)	0.05
μ_c	Co ($2c$)	−1.51
μ_i	Co ($6i$)	−0.65

It would be of interest to relate the local environment of the two nonequivalent Gd sites with the value of the molecular field thereon. Since due to the limited experimental resolution it was not possible to resolve the corresponding two INS peaks, we have to rely on our calculations. These can, indeed, be relied on because the calculated mean value, $\frac{1}{2}(B_a+B_b)$, has been validated by comparison with the INS data. Turning now to the last column of Table III, we observe that B_a is about 14% higher than B_b. The Gd $1a$ site has more Co neighbors (see Fig. 1 and Table II), some of which are the high-spin Co($2c$). This leads to the larger molecular field on Gd $1a$. In contrast, Gd $1b$ has six boron atoms and none of Co($2c$) among its near neighbors, hence the lower molecular field. These results show clearly the influence of the local atomic environment on the magnitude of the molecular field on the Gd sites.

Despite the reasonable agreement between the experimental and calculated values in Table III, one nevertheless observes that the calculations overestimate the mean molecular field on Gd by about 10%, which lies outside the 8% experimental error interval. The remaining discrepancy may arise from the orbital magnetic moments of Co neglected in the present calculations.

IV. CONCLUSION

It has been shown by both experiment and theory that the Gd–Co intersublattice exchange interaction undergoes a dramatic reduction upon the substitution of boron for cobalt in $GdCo_5$. The density-functional calculations are in satisfactory agreement with the experimental value of 130(10) T. The decrease mostly results from a reduction of the cobalt magnetic moment. Indeed, the Gd–Co coupling constant is found to be almost the same in both $GdCo_5$ and $GdCo_4B$. In addition, the calculations demonstrate that the two inequivalent Gd lattice sites experience significantly different molecular fields, which is attributable to the different local atomic environments.

ACKNOWLEDGMENTS

This research has been partially supported by the European Community-Access to Research Infrastructure action of the improving Human Potential Programme. This financial support is gratefully acknowledged. The authors are particularly grateful for the neutron facility provided by ISIS at the Rutherford Appleton Laboratory. The work performed at IFW Dresden was financially supported by Deutsche Forschungsgemeinschaft under SFB463/B11.

[1]N. H. Duc, in *Handbook on the Physics and Chemistry of Rare-Earths*, edited by K. A. Gschneidner, Jr. and L. Eyring (North-Holland, Amsterdam, 1997), Vol. 24.
[2]N. H. Duc and D. Givord, J. Magn. Magn. Mater. **151**, L13 (1995).
[3]N. H. Duc, T. D. Hien, D. Givord, J. J. M. Franse, and F. R. de Boer, J. Magn. Magn. Mater. **124**, 305 (1993).
[4]F. Maruyama, J. Alloys Compd. **320**, 7 (2001).
[5]Y. Suzuki, T. Ito, T. Uchida, O. Nashima, N. M. Hong, and H. Ido, J. Appl. Phys. **81**, 5141 (1997).
[6]E. Burzo, I. Creanga, N. Plugaru, V. Pop, and M. Ursu, Rev. Roum. Phys. **33**, 57 (1988).
[7]J. P. Liu, F. R. de Boer, P. F. de Châtel, R. Coehoorn, and K. H. J. Buschow, J. Magn. Magn. Mater. **132**, 159 (1994).
[8]Z. G. Zhao, F. R. de Boer, and K. H. J. Buschow, J. Alloys Compd. **278**, 69 (1998).
[9]J. P. Liu, F. R. de Boer, and K. H. J. Buschow, J. Less-Common Met. **175**, 137 (1991).
[10]M. D. Kuz'min, Yu. Skourski, D. Eckert, M. Richter, K.-H. Müller, K. P. Skokov, and I. S. Tereshina, Phys. Rev. B **70**, 172412 (2004).
[11]J. M. M. Franse and R. J. Radwanski, in *Magnetic Materials*, edited by K. H. J. Buschow (Elsevier, Amsterdam, 1993), Vol. 7.
[12]P. C. M. Gubbens, A. M. van der Kraan, and K. H. J. Buschow, J. Phys. Colloq. **12**, C12 (1988).
[13]P. Tils, M. Loewenhaupt, K. H. J. Buschow, and R. S. Eccleston, J. Alloys Compd. **289**, 28 (1999).
[14]P. Tils, M. Loewenhaupt, K. H. J. Buschow, and R. S. Eccleston, J. Magn. Magn. Mater. **210**, 196 (2000).
[15]O. Isnard, A. Sippel, M. Loewenhaupt, and R. Bewley, J. Phys.: Condens. Matter **13**, 1 (2001).
[16]O. Isnard, M. Loewenhaupt, and R. Bewley, Physica B **350** E31 (2004).
[17]A. Sippel, L. Jahn, M. Loewenhaupt, D. Eckert, P. Kerschl, A. Handstein, K.-H. Müller, M. Wolf, M. D. Kuz'min, L. Steinbeck, M. Richter, A. Teresiak, and R. Bewley, Phys. Rev. B **65**, 064408 (2002).
[18]M. D. Kuz'min, L. Steinbeck, and M. Richter, Phys. Rev. B **65**, 064409 (2002).
[19]M. Liebs, K. Hummler, and M. Fähnle, J. Magn. Magn. Mater. **124**, 239 (1993).
[20]M. S. S. Brooks and B. Johansson, in *Magnetic Materials*, edited by K. H. J. Buschow (Elsevier, Amsterdam, 1993), Vol. 7.
[21]Y. B. Kuz'ma and N. S. Bilonizhko, Sov. Phys. Crystallogr. **18**, 447 (1974).
[22]H. Ogata, H. Ido, and H. Yamauchi, J. Appl. Phys. **73**, 5911 (1993).
[23]E. Burzo, J. Magn. Magn. Mater. **140–144**, 2013 (1995).
[24]C. Zlotea, C. Chacon, and O. Isnard, J. Appl. Phys. **92**, 7382 (2002).
[25]C. Chacon and O. Isnard, J. Phys.: Condens. Matter **13**, 5841 (2001).
[26]N. A. ElMasry, H. H. Stadelmaier, C. J. Shahwan, and L. T. Jordan, Z. Metallkd. **74**, 33 (1983).
[27]R. Ballou, E. Burzo, and V. Pop, J. Magn. Magn. Mater. **140–144**, 945 (1995).
[28]Euriso-Top S. A. (http://www.eurisotop.fr).
[29]A. D. Taylor, B. C. Boland, Z. A. Bowden, and T. J. L. Jones, Rutherford Appleton Laboratory Report No. RAL-87-012, 1987.
[30]M. Liebs, K. Hummler, and M. Fähnle, Phys. Rev. B **46**, 11201 (1992).
[31]K. Koepernik and H. Eschrig, Phys. Rev. B **59**, 1743 (1999).
[32]J. P. Perdew and Y. Wang, Phys. Rev. B **45**, 13244 (1992).
[33]M. T. Czyżyk and G. A. Sawatzky, Phys. Rev. B **49**, 14211 (1994).
[34]C. Chacon and O. Isnard, J. Solid State Chem. **154**, 242 (2000).
[35]A. T. Pedziwiatr, S. Y. Jiang, W. E. Wallace, E. Burzo, and V. Pop, J. Magn. Magn. Mater. **66**, 69 (1987).
[36]C. V. Thang, Ph.D. thesis, University van Amsterdam, 1996.
[37]O. Isnard and C. Chacon Carillo, J. Alloys Compd. **442**, 22 (2007).
[38]C. Chacon and O. Isnard, J. Appl. Phys. **89**, 71 (2001).
[39]A. Kowalczyk, G. Chelkowska, and A. Szajek, Solid State Commun. **120**, 407 (2001).
[40]H. Yamada, K. Terao, H. Nakazawa, I. Kitagawa, N. Suzuki, and H. Ido, J. Magn. Magn. Mater. **183**, 194 (1998).
[41]A. Szajek, J. Magn. Magn. Mater. **185**, 322 (1998).
[42]M. Loewenhaupt, P. Tils, K. H. J. Buschow, and R. S. Eccleston, J. Magn. Magn. Mater. **138**, 52 (1994).